J|A|C|S
ARTICLES

Published on Web 05/15/2008

Effects of Trimethylamine *N*-Oxide (TMAO) and Crowding Agents on the Stability of RNA Hairpins

David L. Pincus,[†] Changbong Hyeon,[§] and D. Thirumalai*[,†,‡]

Biophysics Program, Institute for Physical Science and Technology, and Department of Chemistry and Biochemistry, University of Maryland, College Park, Maryland 20742, and Department of Chemistry, Chung-Ang University, Seoul 156-756, Republic of Korea

Received October 31, 2007; E-mail: thirum@glue.umd.edu

Abstract: We study the effect of the osmolyte, Trimethylamine *N*-Oxide (TMAO), which accumulates in cells in response to osmotic stress, on the stability of RNA hairpins. All atom molecular dynamics (MD) simulations of a nucleotide and the 22-nucleotide RNA hairpin P5GA in an aqueous TMAO solution show that TMAO preferentially interacts with the base through the formation of a single hydrogen bond. To circumvent the difficulties of adequately sampling the conformational space of polynucleotides, we used coarse-grained models (including one that is inspired by the results of all-atom MD simulations of a single nucleotide) to probe the effects of osmoyltes on the stability of P5GA. If, as revealed by our MD simulations, the cosolute specifically interacts with only one base at a time, then we find practically no change in hairpin stability as measured by $\Delta T_m = T_m(\Phi) - T_m$, where $T_m(\Phi)$ and T_m are the melting temperatures at volume fraction Φ of the osmolyte and $\Phi = 0$, respectively. This finding is in *qualitative* agreement with recent experiments. If the interactions between the RNA and osmolytes are repulsive, which is appropriate for mimicking the effects of crowding, ΔT_m can vary from 5 to 15 K depending on the size of the osmolyte and the nature of RNA−osmolyte interactions. Cosolutes that interact favorably with multiple bases simultaneously can stabilize the hairpin more than a crowding agent of the same size. The implications of our predictions for experiments are briefly outlined.

1. Introduction

It is known,[1,2] but not widely appreciated, that the regulation of organic osmotic solvent (osmolyte) concentration helps organisms combat environmental stresses such as elevated temperatures, desiccation, or the presence of urea. For example, trimethylamine *N*-oxide (TMAO) counteracts the presence of urea in kidneys to prevent renal diseases. More generally, the pioneering studies by Somero and co-workers[3,1] showed that, in all taxa, the concentration of osmolytes have been adjusted by convergent evolution to cope with environmental stresses without compromising the functions of biological macromolecules. The term *osmolyte* derives from cellular response to the osmotic stress of a high salinity environment (e.g., the ocean). Most osmolytes, such as urea, destabilize proteins and RNA,[4] whereas TMAO is an example of a protecting osmolyte.

The majority of studies focused on the effects of osmolytes on the stability of proteins. From general physical considerations, two extreme scenarios can be envisioned for the effect of osmolytes on the stability of proteins and RNA. If osmolytes interact directly with the protein surface the folded state would be destabilized at sufficiently high solute concentrations. Direct interaction with proteins occurs if the preference for osmolyte exceeds that for water. It is now established, after decades of research,[5,6] that urea and guanidinium hydrochloride[7–11] denature proteins by preferentially binding to the protein backbone.

In contrast, if osmolyte is depleted from the vicinity of proteins, then the stability of the native state is enhanced by an entropic stabilization mechanism.[12–14] The TMAO-induced enhancement of protein stability is due to its depletion near the protein surface (i.e., the local density of TMAO around proteins is less than in the bulk). This mechanism is most appropriate when the dominant interactions between the osmolyte and the biomolecule are due to excluded volume, and when the global structure of compact conformations of the protein in the native basin of attraction (NBA) are not greatly altered. Entropic

[†] Biophysics Program, Institute for Physical Science and Technology, University of Maryland.
[‡] Department of Chemistry and Biochemistry, University of Maryland.
[§] Chung-Ang University.

(1) Yancey, P. H.; Clark, M. E.; Hand, S. C.; Bowlus, D.; Somero, G. *Science* **1982**, *217*, 1214–1222.
(2) Record, M. T., Jr.; Courtenay, E. S.; Cayley, D. S.; Guttman, H. J. *TIBS* **1998**, *23*, 143–148.
(3) Yancey, P. H.; Somero, G. N. *Biochem. J.* **1979**, *183*, 317–323.
(4) Pan, J.; Thirumalai, D.; Woodson, S. A. *J. Mol. Biol.* **1997**, *273*, 7–13.
(5) Robinson, D. R.; Jencks, W. P. *J. Am. Chem. Soc.* **1965**, *87*, 2462–2470.
(6) Schellman, J. A. *Biophys. Chem.* **2002**, *96*, 91–101.
(7) Wallqvist, A.; Covell, D. G.; Thirumalai, D. *J. Am. Chem. Soc.* **1998**, *120*, 427–428.
(8) Auton, M.; Holthauzen, L. M. F.; Bolen, D. W. *Proc. Natl. Acad. Sci. U.S.A.* **2007**, *104*, 15317–15322.
(9) O'Brien, E. P.; Dima, R. I.; Brooks, B.; Thirumalai, D. *J. Am. Chem. Soc.* **2007**, *129*, 7346–7353.
(10) Rezus, Y. L. A.; Bakker, H. J. *Proc. Natl. Acad. Sci. U.S.A.* **2006**, *103*, 18417–18420.
(11) Zou, Q.; Habermann-Rottinghaus, S. M.; Murphy, K. P. *Proteins: Struct., Funct., Genet.* **1998**, *31*, 107–115.
(12) Minton, A. P. *Curr. Opin. Struct. Biol.* **2000**, *10*, 34–39.
(13) Ellis, R. J. *Curr. Opin. Struct. Biol.* **2001**, *11*, 114–119.
(14) Minton, A. P. *Biophys. J.* **2005**, *88*, 971–985.

10.1021/ja078326w CCC: $40.75

stabilization is invoked to explain the enhanced stability of proteins in the presence of any species which occupies a significant fraction of a solution's available volume.[14–16] The conformations in the unfolded basin of attraction (UBA) can sample extended structures, e.g., as measured by the radius of gyration (R_g). However, the finite volume occupied by osmolytes (or more generally crowding agents) decreases the probability of extended states being sampled, thus decreasing the entropy associated with the UBA. In turn, the reversible work required to unfold the protein increases. Thus, the volume excluded by the osmolytes shifts the NBA $\rightleftharpoons$ UBA equilibrium toward the more compact NBA. Osmolytes, which experience unfavorable interactions with a protein backbone (e.g., TMAO), are thought to shift the folding equilibrium toward the NBA. This follows because the polypeptide backbone of structures in the NBA is at least partially buried and thereby minimizes unfavorable interactions with the osmolytes. Thus, one can think of the depletion of osmolytes around a biopolymer as introducing an effective attraction between monomers.[16,17] The entropic stabilization mechanism is fairly general and depends only on the volume fraction of osmolytes, Φ, which can be altered by changing either the density of the osmolyte and/or its specific volume. When the size of the osmolyte becomes comparable to that of the biomolecule a substantial fraction of the solution's volume is excluded even when Φ is small.

The effect of osmolytes on the stability of RNAs (e.g., tRNA, RNA hairpins, and ribozymes) is of interest because any alterations in their stability can profoundly affect a number of cellular functions ranging from gene expression to transcription to splicing reactions. Despite its importance, not much is known about osmolyte−RNA interactions at the molecular level. The scenarios outlined above show that denaturing osmolytes engage in direct interaction with proteins while renaturing osmolytes are depleted from their surface. Similar considerations also apply to highly charged RNA, despite the differences in the driving forces for ordered structure formation in proteins and nucleic acids. The general scenarios, however, do not provide a molecular picture of the mechanism of stabilization (or destabilization), which requires either simulations or NMR experiments that probe local interactions.

Two recent studies have examined osmolyte effects on the stability of folded RNA molecules. Gluick and Yadav[18] observed a shift of $\sim$25 K in the Φ-dependent melting temperature, $T_m(\Phi)$, of a tRNA molecule with the increasing concentration of TMAO (the increase is approximately 5 K in the presence of 1 M TMAO). They associated the increase in T_m over the bulk $T_m(\Phi = 0)$ with TMAO-induced enhancement of the tertiary structure of tRNA. In contrast, their study suggested very little, if any, change in the melting temperature of secondary structures.

In an important paper, Lambert and Draper (LD)[19] carried out systematic experiments on the effect of a number of osmolytes on RNA molecules of varying architecture. LD showed that almost all the osmolytes, including urea and TMAO which have opposing effects on protein stability, destabilized a 16-nt RNA hairpin. The extent of destabilization depends on the nature of the osmolyte. For example, $\Delta T_m = T_m(\Phi) - T_m(0)$, is quite small ($\approx -0.5$ K) at 1 molal TMAO concentration. In contrast, tertiary interactions are stabilized by most of the osmolytes used in their study. LD hypothesized that destabilization of secondary structures is a result of preferential accumulation of osmolytes around the base groups and depletion around the ribose−phosphate backone. Although osmolytes are preferentially excluded from the RNA backbone, the backbone is not buried in RNA secondary structures. When RNA folds into its native tertiary structure, however, some of the sugar−phosphate backbone is buried. Thus, depletion of osmolytes around the backbone stabilizes the tertiary structure, which apparently compensates for the destabilization of the secondary structures.

In this paper, we have carried out a range of computational studies to provide further insights into the nature of molecular interactions (in the presence of osmolytes) that control the stability of RNA hairpins. Using a combination of all-atom molecular dynamics (MD) and Langevin simulations of a coarse-grained model for an RNA hairpin, we show that the preferential interaction of TMAO with the bases results in minor changes in T_m as compared to the bulk. The all-atom simulations of 5′ Guanosine Monophosphate (5GP) reveal an enhanced density of TMAO around the guanine base, confirming the plausibility of secondary structure destabilization as hypothesized by LD. The results of the MD simulations were used to construct a number of coarse-grained models to probe the effects of TMAO and crowding agents on the stability of P5GA, a 22-nucleotide (nt) RNA hairpin. If specific attractive interactions between the cosolute and the base are included, as revealed by our MD simulations, we find a small shift in the melting temperature, which shows that the stability of the RNA hairpin is not significantly altered by TMAO. In the entropic stabilization limit, which is realized by modeling TMAO as spheres, our simulations show that the extent of hairpin stabilization in 1 M TMAO solution is relatively small ($\Delta T_m \approx 4.5$ K). Additional stability results when osmolytes are capable of engaging in multiple attractive interactions with base groups $\Delta T_m \approx 10.5$ K. Such a model might explain the effects of glycerol on select RNA structures. Our results suggest that specific interactions are vital for understanding osmolyte effects on RNA secondary structure because their magnitude is comparable to the universally present entropically induced intramolecular depletion attraction. Finally, we predict that depletion effects on RNA secondary structure are substantially greater in the presence of larger cosolutes (or crowding agents), i.e., those cosolutes that avoid the surface of RNA.

2. Methods

All Atom Molecular Dynamics (MD) Simulations. We placed a single nucleotide, 5′ Guanosine Monophosphate (5GP, see Figure 1A), in a cubic box along with 12 TMAO molecules, 3 sodium ions, 1 chloride ion, and 525 TIP3P waters. This corresponds to a TMAO concentration of approximately 1.2 M. There were a total of 1783 atoms in the MD simulations of 5′ guanosine monophosphate (initial structure retrieved from HIC-Up database,[20] residue name 5GP), whose interactions were governed by the CHARMM27 force field.[21]

(15) Cheung, M. S.; Klimov, D.; Thirumalai, D. *Proc. Natl. Acad. Sci. U.S.A.* **2005**, *102*, 4753–4758.
(16) Shaw, M. R.; Thirumalai, D. *Phys. Rev. A* **1991**, *44*, R4797−R4800.
(17) Asakura, S.; Oosawa, F. *J. Chem. Phys.* **1954**, *22*, 1255–1256.
(18) Gluick, T. C.; Yadav, S. *J. Am. Chem. Soc.* **2003**, *125*, 4418–4419.
(19) Lambert, D.; Draper, D. E. *J. Mol. Biol.* **2007**, *370*, 993–1005.
(20) Kleywegt, G. J.; Jones, T. A. *Acta Crystallogr., Sect. D* **1998**, *54*, 1119–1131.
(21) Brooks, B. R.; Bruccoleri, R. E.; Olafson, B. D.; States, D. J.; Swaminathan, S.; Karplus, M. *J. Comput. Chem.* **1983**, *4*, 187–217.
(22) Kast, K. M.; Brickmann, J.; Kast, S. M.; Berry, R. S. *J. Phys. Chem. A* **2003**, *107*, 5342–5351.

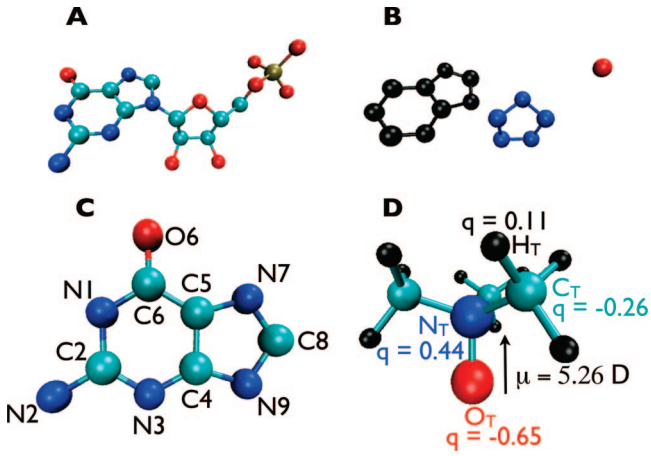

Figure 1. (A) Ball and stick representation of 5′ Guanosine Monophosphate (5GP). Only heavy atoms are rendered. Carbon atoms are colored cyan; nitrogen atoms are blue; oxygen atoms are red; and the phosphorus atom is tan. (B) For the purposes of Figure 2, the position of the 5GP base and sugar moieties are defined by the centers of geometry of their ring heavy atoms (colored black and blue, respectively). The position of the phosphate group corresponds to that of its central phosphorus atom (colored red). (C) Heavy atoms of the guanine base. The labels correspond to those used in Figure 3. (D) Trimethylamine *N*-oxide (TMAO) consists of a central nitrogen atom (colored blue) surrounded by an oxygen atom (colored red) and three methyl groups (carbon atoms colored cyan, and hydrogens colored black). The values of the partial charges on all TMAO atom-types are given. The dipole moment associated with the distribution of charge indicated has a magnitude of 5.26 D and lies along the O_T-N_T bond vector. The figures were produced with VMD. [43]

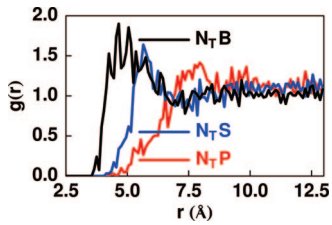

Figure 2. Radial distribution functions for N_T-Base (B), N_T-Sugar (S), and N_T-Phosphate (P) separations. The base, sugar, and phosphate positions with respect to which $g(r)$'s are computed are defined as in Figure 1B. The excess TMAO density around the 5GP base is both greater and found at shorter distances than the density around either the sugar or phosphate groups.

The parameters for the TMAO force field were obtained from Tables 2, 3, 4, 7, and 8 of Kast et al.[22] Certain TMAO parameters required slight adjustment to conform to the CHARMM functional form. The force constants for bond stretching, angle bending, and Urey−Bradley stretching were scaled by a factor of 0.5 from their values in Kast et al. The Lennard−Jones (LJ) collision diameters were also modified; Kast et al. used $V_{LJ}(r) = 4\varepsilon[(\sigma/r)^{12} - (\sigma/r)^6]$, while CHARMM uses $V_{LJ}(r) = \varepsilon[(r_{min}/r)^{12} - 2(r_{min}/r)^6]$ where $r_{min} = 2^{1/6}\sigma$. Note that the atom types O_T, N_T, C_T, and H_T, respectively, correspond to atom types ON1, NN1, CT3N1, and HAN1 in Kast et al. The bond stretching force constants, k_b, between the bonded atoms in TMAO (in units of kcal/mol·Å^2) were 171.29 (O_TN_T), 128.085 (N_TC_T), and 295.48 (C_TH_T), where throughout this paper we use the subscript T for TMAO. The values of (ε_α, $r^\alpha_{min}/2$) with α being the atom type were (−0.1526, 1.832981) for O_T, (−0.2, 1.642162) for N_T, (−0.0676, 1.706704) for C_T, and (−0.0185, 0.996185) for H_T. We express ε_α in units of kcal/mol and distance in angstroms. The angle bending and Urey−Bradley force constants are given in Table 1.

MD Simulation Details. We performed all-atom simulations at $T = 298$ K using the NAMD2 MD program.[23] A cubic box of length $L = 25.6$ Å resulted from an initial 100 ps of NPT equilibration. After an additional 1 ns of NVT equilibration, we collected data from 10 independent 1 ns trajectories in the NVT ensemble. The number and length of trajectories are sufficient to obtain a detailed picture of the interactions of TMAO with a single base. Samples were collected every 10 ps for a total of 2000 samples. We employ periodic boundary conditions in the MD simulations, and electrostatic interactions were treated using the particle mesh Ewald summation with a 0.91 Å grid spacing. The van der Waals (VDW) interactions were smoothly truncated with a 12.0 Å cutoff and a 10.0 Å switching distance.

The equations of motion were integrated with a 1 fs time step. Bonds involving H-atoms were rigid, while VDW interactions and full electrostatics were calculated at every time step. Pair lists were updated every 10 time steps. Pressure was maintained at $P = 1$ atm using the Nose−Hoover Langevin piston method [24,25] with an oscillation period of 100 fs and a decay time of 50 fs. Temperature was controlled by applying Langevin forces to all heavy atoms with a coupling coefficient of 5 ps^{-1}.

Coarse Grained (CG) Models. The difficulty in using all-atom MD simulations to exhaustively sample conformations, even for small RNA hairpins, makes it necessary to consider alternative methods. In order to obtain converged results for the stability of RNA hairpins as a function of crowding agents and MD-inspired models for TMAO, we used a coarse-grained model of RNA. We performed implicit solvent Langevin Dynamics simulations on a 22-nt hairpin, P5GA (Figure 6), to study osmolyte and crowding effects on the RNA secondary structure. The system is small enough to ensure that our calculations are converged but sufficiently large to capture the interplay between chain entropy and specific TMAO-induced interactions. The smaller P5GA is similar to P5ab in the P5abc domain of the group I intron in that it has a GAAA tetraloop connected to a stem, and its NMR structure has been determined (PDB accession number 1EOR).[26]

Our Langevin simulations employed the three-interaction-site (TIS) model introduced by Hyeon and Thirumalai.[27,28] All sites in this model are of equivalent mass, and each represents a phosphate group, a ribose group, or a base. Thus, an RNA molecule with N nucleotides is represented by $3N$ interaction sites. The P5GA model contained only $3N - 1$ sites; no coordinates exist for the atoms of the first phosphate group.

Osmolytes were represented as spheres with radii $r = 2.7$ Å, corresponding to the radius of TMAO. We also performed a set of simulations using spherical crowding agents with radii $r = 7.0$ Å.

Energy Functions in the CG Models. The total potential energy, V_{tot}, in the CG simulations was a sum of intra- and intermolecular interactions: $V_{tot} = V_{intra} + V_{inter}$. The form of the intramolecular potential, V_{intra}, has been described previously.[27,28] In this work, we employed a salt concentration $c = 100$ mM NaCl implicitly through the Debye−Hückel screened electrostatic potential; this value is half the value found in the header of the 1EOR PDB file.[26]

To explore a range of interactions between the osmolyte and RNA we considered several models. The sets of osmolyte, base, sugar, and phosphate interaction sites are denoted O, B, S, and P, respectively. The interactions between elements of O and elements

(23) Phillips, J. C.; Braun, R.; Wang, W.; Gumbart, J.; Tajkhorshid, E.; Villa, E.; Chipot, C.; Skeel, R. D.; Kale, L.; Schulten, K. *J. Comput. Chem.* **2005**, *26*, 1781–1802.
(24) Martyna, G. J.; Tobias, D. J.; Klein, M. L. *J. Chem. Phys.* **1994**, *101*, 4177–4189.
(25) Feller, S. E.; Zhang, Y.; Pastor, R. W.; Brooks, B. R. *J. Chem. Phys.* **1995**, *103*, 4613–4621.
(26) Rüdisser, S.; Tinoco, I., Jr. *J. Mol. Biol.* **2000**, *295*, 1211–1223.
(27) Hyeon, C.; Thirumalai, D. *Proc. Natl. Acad. Sci. U.S.A.* **2005**, *102*, 6789–6794.
(28) Hyeon, C.; Thirumalai, D. *Biophys. J.* **2006**, *90*, 3410–3427.

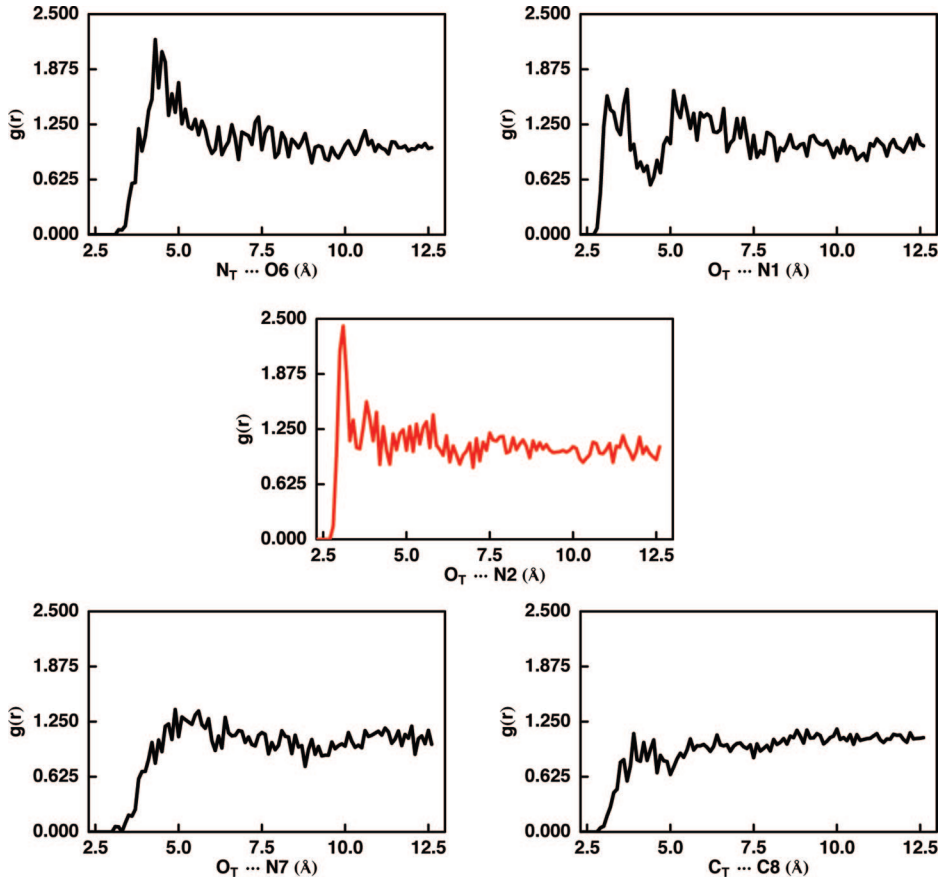

Figure 3. A representative sample of the radial distribution functions between TMAO and heavy atoms of the 5GP base. 5GP atoms are labelled as in Figure 1C. A peak of 2.42 in $g(r)$ associated with $O_T\cdots N2$ separation occurs at $r = 3.1$ Å (central red curve) and is consistent with hydrogen bonding between the pair. All other interactions are weak and longer-ranged (see also Figures 10−12 in the Supporting Information).

Table 1. Angle Bending and Urey−Bradley Force Constants for TMAO[a]

type (a)	type (b)	type (c)	k_θ^{abc}/ kcal mol^{-1} rad^{-2b}	k_{ub}^{ac}/ kcal mol^{-1} Å^{-2c}
O_T	N_T	C_T	30.470	36.010
N_T	C_T	H_T	24.970	78.650
C_T	N_T	C_T	68.850	48.515
H_T	C_T	H_T	27.435	6.565

[a] Parameters taken from Table 8 of Kast et al.[22] but scaled by a factor of 0.5 to conform to the functional form of the CHARMM force field.[21] [b] The angle bending force constant, k_θ^{abc}, depends on the atom types (a), (b), and (c) of the angle. [c] The Urey−Bradley force constant, k_{ub}^{ac}, depends only on atom types (a) and (c) (i.e., the atom types of the 1−3 atoms) of the angle.

of S and P were repulsive, which is in accord with our MD results (see below). The pairwise additive repulsive Soft-Sphere interaction between the osmolytes and other interaction sites was

$$V_{SS}(ij) = \varepsilon_{ij}\left(\frac{\sigma_{ij}}{r}\right)^{12} \tag{1}$$

where i denotes an osmolyte interaction site, j denotes any type of interaction site, r is the separation distance between the i and j interaction sites, and σ_{ij} is the distance at which the potential energy of interaction equals ε_{ij}. Similarly for Lennard−Jones (LJ) interactions between osmolytes and other interaction sites,

$$V_{LJ}(ij) = \varepsilon_{ij}\left[\left(\frac{\sigma_{ij}}{r}\right)^{12} - 2\left(\frac{\sigma_{ij}}{r}\right)^{6}\right] \tag{2}$$

where i denotes an osmolyte interaction site, j denotes any type of interaction site, r is the separation between the i and j interaction sites, σ_{ij} is the distance at which the potential energy of interaction is a minimum, and ε_{ij} is the well-depth.

We consider four different models.

$$V^{HB} = \sum_{i\in O}\sum_{j\in S,P} V_{SS}(ij) + \sum_{i\in O}{\sum_{j\in B}}' V_{LJ}(ij) + \sum_{i\in O}\sum_{\substack{j\in O,\\ j>i}} V_{LJ}(ij) \tag{3}$$

$$V^{ES} = \sum_{i\in O}\sum_{j\in S,P,B} V_{SS}(ij) + \sum_{i\in O}\sum_{\substack{j\in O,\\ j>i}} V_{SS}(ij) \tag{4}$$

$$V^{AC} = \sum_{i\in O}\sum_{j\in S,P,B} V_{SS}(ij) + \sum_{i\in O}\sum_{\substack{j\in O,\\ j>i}} V_{LJ}(ij) \tag{5}$$

$$V^{MS} = \sum_{i\in O}\sum_{j\in S,P} V_{SS}(ij) + \sum_{i\in O}\sum_{j\in B} V_{LJ}(ij) + \sum_{i\in O}\sum_{\substack{j\in O,\\ j>i}} V_{LJ}(ij) \tag{6}$$

(i) The first CG model, V^{HB}, mimicked hydrogen bonding between TMAO and nucleotide bases and derived its inspiration from the results of our MD simulations. The prime on the second summation indicates the restriction that each osmolyte only interacted with the base closest to it. In other words, for each osmolyte the distance to every base site of the hairpin was calculated. The base site corresponding to the minimum distance interacted with the osmolyte site via an LJ potential. The osmolyte did not interact with any other base sites. Thus, just as a single molecule of TMAO is only capable of forming a hydrogen bond with a single base, a single osmolyte in the V^{HB} model could only interact with one base site. (ii) The entropic stabilization mechanism was mimicked using the V^{ES} energy function in which interactions

Table 2. Parameters for Osmolyte−Osmolyte (OO) and Osmolyte−Base (OB) Interactions Used in the Coarse Grained Model (Eqs 1 and 2)[a]

model/osmolyte radius/Å	ε_{OO}/kcal mol^{-1}	σ_{OO}/Å	ε_{OB}/kcal mol^{-1}	σ_{OB}/Å
V^{ES}/ 2.7	1.0	5.4	1.00	4.4
V^{AC}/ 2.7[b]	1.0	5.4	1.00	4.4
V^{MS}/ 2.7[c]	1.0	5.4	1.22	4.4
V^{HB}/ 2.7[d]	1.0	5.4	1.22	4.4
V^{AC}/ 7.0[b]	1.0	14.0	1.00	8.7

[a] In all the models interactions between osmolyte (O) and sugar (S) and phosphate (P) are repulsive. [b] The LJ potential is used only between osmolytes (OO). [c] OO and OB interactions are given by LJ while other interactions are repulsive. [d] Each O only interacts with the *closest* B (via an LJ potential). The LJ potential is also used for all OO interactions. All other interactions are repulsive.

between O and interaction sites on the RNA were repulsive (eq 1). (iii) To probe the effect of weak attraction between the osmolyte particles, we used the V^{AC} model in which the LJ potential was used for OO and all other interactions were repulsive. (iv) Some cosolutes can interact with multiple bases by possibly forming a network of hydrogen bonds. This effect was simulated using the multiple site model, V^{MS}, in which OO and OB interactions were given by the LJ potential while other interactions were repulsive. The parameters (ε, σ) for the always repulsive osmolyte−sugar and osmolyte−phosphate interactions were (1.0 kcal/mol, 4.4 Å). For the crowding agents of radii $r = 7.0$ Å, the values of these (ε, σ) parameters were (1.0 kcal/mol, 8.7 Å). Table 2 provides the remaining parameter values for the various models.

Coarse Grained Simulation Details. The simulations were performed in a cubic box of length $L = 62$ Å with 145 osmolytes. This roughly corresponds to a 1.0 M solution of TMAO and yields a volume fraction $\Phi = \rho(^4/_3\pi r^3) = {}^{145}/_{62^3}(^4/_3\pi(2.7)^3) \approx 0.05$, where $\rho = N/L^3$. Simulations with larger crowding agents (of radii 7.0 Å) employed 1270 spheres in a box of length $L = 230$ Å (corresponding to a density of $\rho \approx 170$ mM). We applied periodic boundary conditions[29] to osmolyte positions, and the minimum image convention[29] was applied to RNA−osmolyte and osmolyte−osmolyte distances.

The potentials in eqs 1 and 2 (see Tables 3 and 4 in the Supporting Information for details) were shifted such that both the potential and force go to zero at a finite cutoff distance yet remain continuous functions of r.[29] The cutoff distances were chosen to ensure that the magnitude of the corresponding unshifted potential at the cutoff decayed to less than $0.001k_BT$. The positions of the minima of the shifted and unshifted potentials do not differ significantly from one another.

We integrated the Langevin equation using a velocity verlet algorithm.[30,31] The mass, m, of an RNA bead ranges from 0.1 to 0.16 kg mol^{-1}. The average distance between beads is $a = 4.6$ Å, and the energy scale, ε_h, is ~1 kcal mol^{-1}. Thus, $\tau_L = (ma^2/\varepsilon_h)^{1/2} \approx 2-3$ ps. We chose the value of the friction coefficient $\zeta = 0.05\tau_L^{-1}$ and the time step $h = 0.0025\tau_L$. The underdamped dynamics results in efficient sampling of the conformational space thus enabling us to obtain converged results for thermodynamic quantities.

Order Parameters and Analysis. Thermodynamic averages of a number of physical quantities were calculated using the multiple histogram technique.[32,33] We computed several physical quantities, including the fraction of native contacts (Q) and the square radius of gyration (R_g^2), to characterize the changes in the osmolyte-induced stability of P5GA.

We used free-energy profiles ($F_\beta(x)$ vs x) to calculate hairpin melting temperatures and the relation $F_\beta(x) \simeq -k_BT \ln P_\beta(X = x)$, where $P_\beta(X = x)$ is the probability distribution function associated with the variable X (here X is either Q or R_g) and $\beta = 1/k_BT$ is the inverse temperature, to generate such profiles. We determined $P_\beta(X = x)$ using the multiple histogram technique. More rigorously, we should write $F_\beta(x) - k_BT \ln Z(\beta) = -k_BT \ln P_\beta(X = x)$. The additive constant $k_BT \ln Z(\beta)$ is not relevant, since such a constant has no effect on the values of $\Delta F_\beta(x_1, x_2) = F_\beta(X = x_1) - F_\beta(X = x_2)$. At the melting temperature, T_m, the free energy profile contains two distinct minima of equal depth.

3. Results and Discussion

Osmolytes can stabilize, destabilize, or have no net effect on RNA secondary structures. Theory predicts that secondary structures should be entropically stabilized when osmolytes are depleted from RNA.[14−16] Osmolyte-induced stabilization of the native state, whose origin is linked to entropic destabilization of the unfolded state,[15] is valid provided that the interactions between RNA and the osmolyte are dominated by a nonspecific excluded volume. Recent experiments, however, reveal mild destabilization of the RNA secondary structures [18,19] (see Table 5 in the Supporting Information). The experimental results can only be attributable to two possible sources: (1) specific interactions between the osmolytes and RNA and/or (2) an osmolyte induced weakening of the screening between charges along the phosphodiester backbone. We used all-atom molecular dynamics simulations of a single nucleotide in a trimethylamine *N*-oxide (TMAO) solution as a guide to provide insights into the nature of nucleotide−TMAO interactions.

Nucleotide Interactions with TMAO at Atomic Resolution. To look for specific strong interactions, we first calculated radial distribution functions (rdf's) between TMAO and the base, sugar, and phosphate moieties of 5GP. The rdf's were computed using the position of the central nitrogen atom in TMAO (Figure 1D). The centers of geometry of the ring atoms of the base and sugar positions were used to compute the rdf's involving 5GP (see Figure 1B). The rdf involving the phosphate group was computed using the position of the central phosphorus atom. The rdf's in Figure 2 show that TMAO preferentially accumulates around the base rather than the sugar or the phosphate. The density of TMAO is both greater and found at a closer distance of approach ($r \approx 4.5$Å) than the densities around the geometric centers of the sugar or the phophate.

To probe the nature of specific interactions further, we calculated the rdf's between all distinct heavy atom types of TMAO and all distinct heavy atom types of 5GP (Figure 1). The resulting rdf's, Figure 3 and Figures 10−12 in the Supporting Information, reveal excess density at a short distance between O_T and N2. A peak of 2.42 in $g_{O_TN2}(r)$ occurs at $r = 3.1$ Å. This peak is associated with a hydrogen bond interaction in which O_T acts as an acceptor and one of the N−H bonds associated with the N2 nitrogen acts as a donor. Since N2 is involved in Watson−Crick base pairing, and since this base pairing helps stabilize the nucleic acid structure, it is not surprising that any cosolute that disrupts such hydrogen bond interactions could potentially destabilize RNA secondary structures. It is important to point out that TMAO can interact *directly with only one base*. This observation has an important consequence on the effect of TMAO on hairpin stability.

(29) Allen, M. P.; Tildesley, D. J. *Computer Simulation of Liquids*; Oxford University Press: 1987.
(30) Klimov, D. K.; Newfield, D.; Thirumalai, D. *Proc. Natl. Acad. Sci. U.S.A.* **2002**, *99*, 8019–8024.
(31) Klimov, D. K.; Thirumalai, D. *Proc. Natl. Acad. Sci. U.S.A.* **2000**, *97*, 2544–2549.
(32) Kumar, S.; Bouzida, D.; Swendsen, R. H.; Kollman, P. A.; Rosenberg, J. M. *J. Comput. Chem.* **1992**, *13*, 1011–1021.
(33) Newman, M. E. J.; Barkema, G. T. *Monte Carlo Methods in Statistical Physics*; Oxford University Press: 2004.

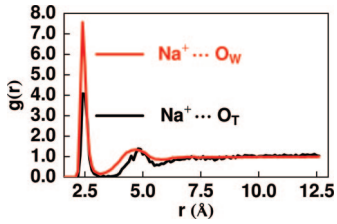

Figure 4. Radial distribution functions associated with $Na^+\cdots$TIP3P water oxygen distance (red curve) and the $Na^+\cdots O_T$ oxygen distance (black curve). There are significantly more first shell waters around the sodium ions.

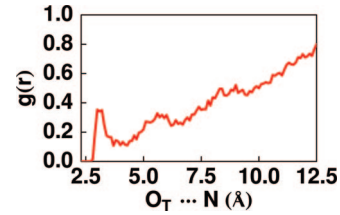

Figure 5. Radial distribution function between TMAO and nitrogen atoms of the $-NH_2$ groups of the guanine (N2), cytosine (N4), and adenine (N6) present in the P5GA hairpin. The rdf is calculated by averaging over the distances between O_T and each of the nitrogen atoms (N2, N4, N6). The results show clear depletion of the TMAO from the nitrogen in stacked conformations of the RNA hairpin at 298 K. The differing accessibility of the hairpin bases in folded and unfolded conformations is important in compensating for the entropic stabilizing forces.

Indeed, this "specific" hydrogen-bonding interaction between osmolyte and base is perhaps more general than might be anticipated. First, all ribonucleotides except for Uridine have similar $-NH_2$ groups attached to the C2 position (Figure 1C) and, hence, can potentially serve as hydrogen-bond donors. Second, all of the osmolytes studied by Lambert and Draper[19] (urea, proline, betaine, sorbitol, sucrose, glycerol, ethylene glycol, methanol, and TMAO) contain functional groups capable of acting as hydrogen bond acceptors. Several of the osmolytes in the LD study are capable of acting as donors as well. Thus, as suggested by LD, the mechanism of destabilization is likely to be similar. The extent of destabilization, i.e., the value of ΔT_m, only depends on the strength of the osmolyte−base interaction. Apparently, proline interacts most strongly with RNA bases while TMAO has the smallest effect. We should stress that the effect of a specific cosolvent on a base will depend on the competition between hydrogen bond formation with water and the base.

A possible weakening of the screening between charges might also explain secondary structure destabilization. As LD mention,[19] however, such effects (if they exist) are extremely small for monovalent salts like NaCl.[34,35] In order to rule out such a possibility, we computed $g(r)$'s between sodium and the oxygen of TMAO with that between Na^+ and the oxygen of water (Figure 4). Despite the similar peak locations, the much larger first peak in water suggests that potential effects of TMAO on ionic screening may be less relevant than specific interactions with the bases.

Base Stacking Affects TMAO Radial Distribution Function. If the enthalpy of TMAO−nucleotide binding is the same in either single-stranded or helical RNA, then the RNA will still experience excluded volume effects of an entropic origin. These effects would stabilize the hairpin. Thus, the greater accessibility of the bases in a denatured or partially denatured RNA conformation is important in offsetting the entropic forces present. Stacking of nucleotides in a secondary structure affects the TMAO radial distribution around the $-NH_2$ group. In order to assess the effects of base stacking, we simulated the RNA P5GA hairpin in atomic detail at 298 K for 5 ns and sampled configurations every 5 ps. From these results we calculated the rdf between O_T and N2, N4, or N6 (N4 and N6 are the Cytosine and Adenine analogues of Guanine's N2). The results (Figure 5) reveal that O_T is highly depleted from the $-NH_2$ moieties in the folded state of the hairpin.

The results of the MD simulations support the LD[19] hypothesis that the preferential accumulation of osmolyte around the base groups destabilizes the RNA secondary structure. Our MD simulations only suffice to demonstrate *plausibility* and are not conclusive largely because the MD simulations were performed on a single nucleotide and not on a polynucleotide with a well-defined secondary structure. Performing similar simulations on P5GA would require several microseconds of simulations to obtain sufficient sampling. To circumvent this difficulty we used Langevin simulations, which allow us to propose models for TMAO−RNA interactions that are, in part, inspired by detailed simulations on a single nucleotide. More generally, the coarse-grained models also allow us to explore crowding effects on the stability of RNA hairpins.

MD-Inspired Specific Interaction V^{HB} Model for Osmolyte−RNA Interactions. The MD simulations show that a single molecule of TMAO forms a single hydrogen bond with N2 of the base (Figure 3). It is also clear that TMAO interacts specifically with only one base at a time, since only its oxygen atom is capable of participating in a hydrogen bond.

These main results were used to construct a coarse-grained model in which the spherical osmolyte, whose size corresponds to TMAO, interacts with only the closest base. While the attractive osmolyte−base interaction in this model was given by eq 2, the potentials between osmolytes and the sugar and phosphate sites were repulsive. Osmolytes interacted with one another via a Lennard−Jones potential (eq 2). To quantify the extent of stabilization, we calculated $\Delta T_m = T_m(\Phi = 0.05) - T_m(\Phi = 0.00)$. For this model, the differences in the thermal averages in the presence and absence of osmolytes are negligible (Figure 7). Furthermore, free energy profile calculations and $d\langle R_g^2\rangle/dT$ maxima (Figure 8 and Supporting Information) yield a $\Delta T_m \approx 2-3$ K. The estimate of ΔT_m obtained from the condition $\langle Q\rangle(T_m) = 0.5$ is only 1.2 K. Thus, when the specific osmolyte−base interaction is mimicked approximately, we find a negligible effect on the melting temperature. It is likely that if the anisotropy in the TMAO−base interaction is included, the ΔT_m may well be small and negligible as observed in the LD experiments. It should be stressed that LD only observed $\Delta T_m = -0.5$ K at 1 molal concentration of TMAO which is in rough accord with our conclusion that TMAO has only a negligible effect on RNA secondary structures.

Entropic Stabilization, Models V^{ES} and V^{AC}. If the interactions between the nucleotides and osmolytes are purely repulsive, we expect osmolyte-induced stabilization of P5GA by an entropic mechanism. The entropic stabilization limit was mimicked using a repulsive potential, eq 1, between osmolytes and the RNA. Osmolyte−osmolyte interactions were taken to be purely repulsive (Model V^{ES}) or assumed to be given by a Lennard−Jones (LJ) potential (Model V^{AC}).

(34) Spink, C. H.; Chaires, J. B. *Biochemistry* **1999**, *38*, 496–508.
(35) Nordstrom, L. J.; Clark, C. A.; Anderson, B.; Champlin, S. M.; Schwinefus, J. J. *Biochemistry* **2006**, *45*, 9604–9614.

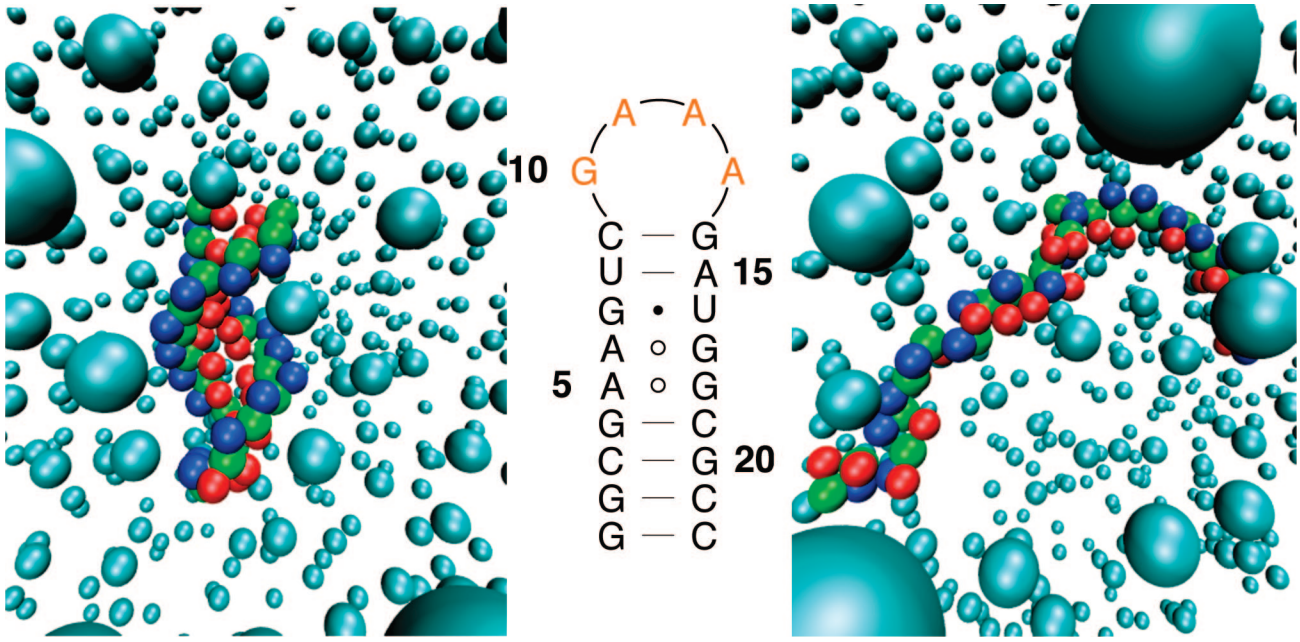

Figure 6. P5GA sequence (center) along with the Three Interaction Site (TIS) model of P5GA in 1.0 M TMAO solution (for the coarse-grained model V^{AC}) at a temperature of 262 K (left) and 373 K (right). Nucleotide bases are colored red, sugars are colored green, and phosphate groups are colored blue. Figures produced with VMD.[43]

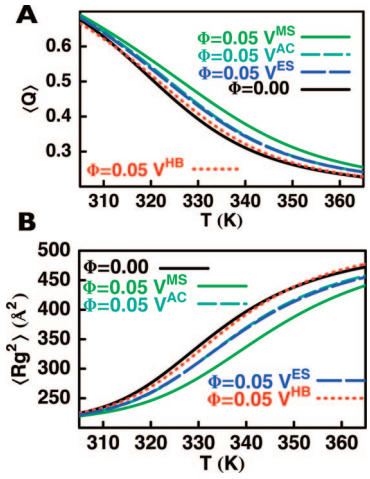

Figure 7. (A) Comparison of thermal average fraction of native contacts ($\langle Q \rangle$) as a function of temperature (T) for various coarse-grained models. The black solid curve corresponds to $\langle Q \rangle$ in the absence of osmolyte (volume fraction $\Phi = 0.00$). The green solid curve (model V^{MS}) demonstrates that $\langle Q \rangle(T)$ can actually increase when osmolytes are capable of forming simultaneous attractive interactions with multiple base sites. Finally, the red-dotted curve reveals that $\langle Q \rangle(T)$ returns to nearly zero-osmolyte behavior when a hydrogen-bond mimicking interaction between osmolyte and base is introduced (model V^{HB}). (B) Examination of $\langle R_g^2 \rangle$ vs T confirms the conclusions drawn from part A.

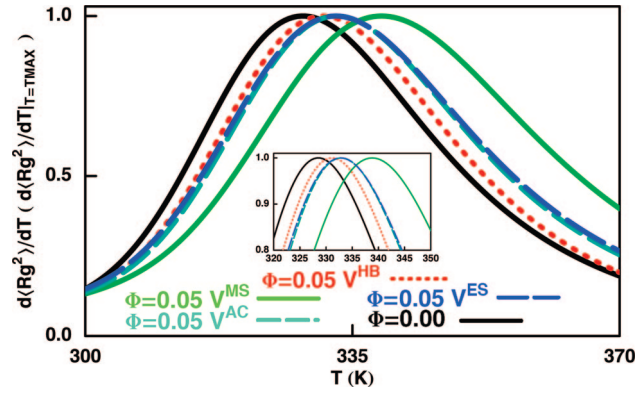

Figure 8. Dependence of $d\langle R_g^2 \rangle/dT$ (normalized by its maximum value) as a function of temperature T. ΔT_m's are determined from shifts in the peak of $d\langle R_g^2 \rangle/dT$ relative to its value in the absence of osmolyte (solid black curve). Model V^{HB} results in the smallest increase of ~3 K, while model V^{MS} results in the largest increase of ~10.5 K. The remaining two entropic models yield increases of ~4.5 K. The inset provides a close-up of the peaks to allow the reader to verify ΔT_m's for the various models.

We used Q, the number of intact base−base native contacts present in a given hairpin conformation, as an order parameter for monitoring hairpin melting. A plot of $\langle Q \rangle$ vs T demonstrates that (on average) more contacts are made in the presence of osmolyte than in their absence (compare either dashed blue curve with the solid black curve in Figure 7A). As a second order parameter, we calculated R_g^2, the square radius of gyration of the hairpin. In the entropic limit, a plot of $\langle R_g^2 \rangle$ vs T also suggests stabilization in the presence of osmolytes. As temperature increases, the $\langle R_g^2 \rangle(\Phi = 0.05) < \langle R_g^2 \rangle(\Phi = 0.00)$ (compare either dashed blue curve with the solid black curve in Figure 7B). To determine the melting temperatures we calculated free energy profiles, $F(Q)$ vs Q, every 0.5 K for all temperatures between 262 and 372 K. The melting temperature, T_m, corresponded to the profile in which the two basins have equal depth (Supporting Information). In the entropic limit $\Delta T_m \approx 5$ K. We also calculated melting temperatures by determining the temperature at which $d\langle R_g^2 \rangle/dT$ has a maximum from which we find $\Delta T_m \approx 4.5$ K (compare either dashed blue curve with the solid black curve in Figure 8). Thus, using reasonable size ($r =$ 2.7 Å) osmolytes at an experimentally relevant density ($\rho =$ 1.0 M), it is clear that the amount of entropic stabilization imparted to an RNA hairpin will be small ($\Delta T_m \approx 4$ or 5 K).

Nonspecific Osmolyte−Base Multiple-Site Interaction, Model V^{MS}. In order to investigate the effects on hairpin stability of energetically favorable osmolyte−base interactions, we introduced an LJ potential between osmolyte and base interaction sites (eq 2). All other interactions between RNA sites and osmolytes were repulsive. Osmolytes interacted with one another

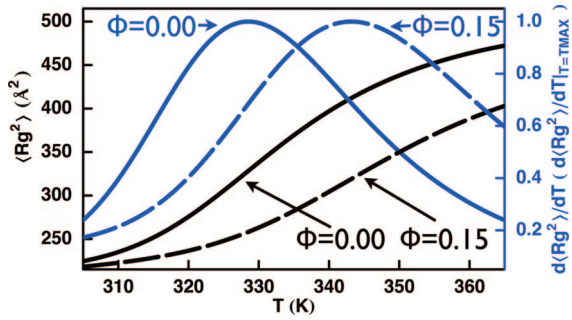

Figure 9. Temperature dependence of $\langle R_g^2 \rangle$ and its derivative. The values of $\langle R_g^2 \rangle$ are in Å^2, and $d\langle R_g^2 \rangle/dT$ is normalized by its maximum value. Entropic stabilization occurs in the presence of crowding agents with radii = 7.00 Å, which is more than twice the size of TMAO. Even at a density of 170 mM (dashed curve; corresponds to a volume fraction $\Phi = 0.15$), the presence of such molecules increases the hairpin T_m by 15 K over its value in the absence of osmolyte (solid curve). This corresponds to roughly 3 times the T_m increase in the presence of smaller ($r = 2.7$ Å) osmolytes at 1 M density.

via an LJ potential. Interestingly, such interactions further stabilized the hairpin. Figure 7 demonstrates that $\langle Q \rangle$ increases and $\langle R_g^2 \rangle$ decreases from their respective values in the entropic limit (compare the solid green curve with either dashed blue curve in the figures). Furthermore, our free energy profile calculations (Supporting Information) suggest that $\Delta T_m \approx 10$ K and $d\langle R_g^2 \rangle/dT$ calculation (Figure 8) confirms that $\Delta T_m \approx 10.5$ K.

Effects of Osmolyte Size. We anticipate that entropic stabilization would play a more important role in the presence of larger and more inert molecules. Because of their size such cosolutes cannot approach close enough to RNA to engage in specific interactions. Preliminary evidence for such behavior is presented in Figure 9. We employed spherical molecules with radii, $r = 7.00$ Å, a 170 mM density, and a volume fraction $\Phi = 0.15$. The results show that in the entropic limit thermal averages are affected to an even greater extent than with the smaller osmolytes. Furthermore, $\Delta T_m \approx 15$ K, roughly 3 times the corresponding $\Delta T_m \approx 5$ K observed in the presence of smaller osmolytes at a higher density. This finding is consistent with expectations based on the entropic stabilization mechanism.[15]

4. Conclusions

To understand the effect of TMAO on the stability of RNA secondary structures, we have carried out a variety of simulations. Not only have these results given insights into the plausible mechanism of TMAO−RNA interaction, but they also provide a basis for interpreting the effects of small crowding agents on the stability of hairpins. There are a number of conclusions and implications of this work that we outline below.

• The all-atom MD simulations show that a single TMAO molecule can preferentially interact with only a single nucleotide through hydrogen bond formation. If TMAO experiences a purely repulsive effective interaction with RNA, then the entropy of the ternary complex (RNA, osmolyte, and solvent) will be greatest when the RNA is compact. On the other hand, if TMAO can accumulate at the RNA surface and there are differences in TMAO accessibility in single stranded, partially folded, and native RNA, then favorable enthalpic interactions can offset the entropic forces favoring the compact structures. In proteins, the most logical site for TMAO interaction is the NH group of the backbone. However, the backbone is shielded from the solvent in the folded states and most likely even when the protein is unfolded. As a result, TMAO is depleted from the protein surface, which in turn leads to its stabilization.[36,37,39] A similar argument was suggested by LD to rationalize the enhanced stability of the RNA tertiary structure. In this case the bases are shielded from the solvent, and hence TMAO cannot engage in hydrogen bond formation with the bases. This is not the case for RNA secondary structures (or partially folded RNA), which enables molecules of TMAO to form single hydrogen bonds with the bases that can destabilize the hairpin. Indeed, our MD simulations revealed that TMAO can only engage in attractive interaction with the closest base.

Using the data in the Supporting Information from Lambert and Draper,[19] we find that destabilization of the 16 nt hairpin used in their study results in a ΔT_m of ~ -0.5 K in the presence of 1 molal TMAO. We also computed ΔT_m for the hairpin in the presence of all other osmolytes used in the LD study (see Table 3 in the Supporting Information). TMAO minimally destabilizes the hairpin, while proline has the largest effect with $\Delta T_m = -3.5$ K at 1 molal proline concentration. It should be stressed that ΔT_m is likely to be much smaller than the width of the transition from which one can only conclude, in accord with our simulations, that TMAO has a negligible effect on hairpin stability. Furthermore, Gluick and Yadav[18] did not discern any change in the T_m of the RNA secondary structure in the presence of TMAO. All of these obervations and our simulations suggest that osmolyte effects on the RNA secondary structure are likely to be small and *specific hydrogen bond interactions are likely to play an important role*.

• Realistic osmolyte size (similar to that of TMAO) and density (≈ 1.0 M) leads to only a small entropic stabilization ($\Delta T_m \approx 4$ or 5 K). Increased stability can result from osmolytes that are capable of simultaneously making energetically favorable interactions with multiple sites on the RNA. Our multiple-site model, V^{ms}, underscores the possibility that any cosolute that can simultaneously engage in hydrogen bond formation with multiple bases or sugars can further stabilize RNA secondary structures. Furthermore, the V^{ms} model predicts a $\Delta T_m = 10.5$ K, which is in rough agreement with the shifts in BWYV secondary structure T_m's in a glycerol solution.[19] Not only is glycerol capable of making multiple simultaneous hydrogen bonds with RNA, but its hydroxyl groups are capable of acting as both donor and acceptor. These properties may allow glycerol to rectify thermal fluctuations responsible for unfolding the hairpin. Lambert and Draper note that this interaction likely does not involve two bases but, rather, a network of minor groove hydrogen bonds.[40] It is intriguing that none of the other molecules with the capability of simultaneously forming multiple hydrogen bonds (e.g., ethylene glycol) resulted in this type of secondary structure stabilization in Lambert and Draper's work.[19]

• Our coarse-grained Langevin dynamics results with larger inert molecules lead us to predict that the size of the osmolyte plays an important role in the stability of the RNA secondary

(36) Liu, Y.; Bolen, D. W. *Biochemistry* **1998**, *34*, 12884–12891.
(37) Bolen, D. W.; Baskakov, I. V. *J. Mol. Biol.* **2001**, *310*, 955–963.
(38) Street, T. O.; Bolen, D. W.; Rose, G. D. *Proc. Natl. Acad. Sci. U.S.A.* **2006**, *103*, 13997–14002.
(39) Street, T. O.; Bolen, D. W.; Rose, G. D. *Proc. Natl. Acad. Sci. U.S.A.* **2006**, *103*, 13997–14002.
(40) Rypniewski, W.; Vallaza, M.; Perbandt, M.; Klussmann, S.; Delucas, L. J.; Betzel, C.; Erdmann, V. A. *Acta Crystallogr., Sect. D* **2006**, *62*, 659–664.

structure. In order to engage in specific interactions with the RNA bases, the size of the cosolute has to be small enough so that short-range ($\approx 3-4$ Å) contacts are possible. TMAO can apparently form hydrogen bonds as evidenced by a sharp peak in $g_{O_TN2}(r)$ in Figure 3. If the cosolute size is sufficiently large to prevent such interactions, then it is likely that they would stabilize, rather than destabilize, RNA secondary structures. It is possible that crowding agents, such as Ficoll or moderate sized PEG, may be a good candidate for such studies.[13,14,41,42]

• The physical principles underlying the mechanism of TMAO interaction with proteins and RNA are similar. In both cases TMAO can form specific hydrogen bonds with sites on RNA or proteins. In RNA, the logical sites are located in the bases given the depletion around sugar and phosphate. The backbone in proteins is shielded effectively so that TMAO cannot form favorable interactions. Potential attractive interactions between TMAO and polar residues are apparently not strong enough. Thus, in both RNA and proteins it is the "accessible surface" that dictates the response to TMAO.

(41) Minton, A. P. J. *Pharm. Sci.* **2005**, *94*, 1668–1675.
(42) Kozer, N.; Kuttner, Y. Y.; Haran, G.; Schreiber, G. *Biophys. J.* **2007**, *92*, 2139–2149.
(43) Humphrey, W.; Dalke, A.; Schulten, K. *J. Mol. Graph.* **1996**, *14*, 33–38.

Acknowledgment. We are grateful to Dr. Sam Cho for useful comments. D.L.P., a Ruth L. Kirschstein Postdoctoral Fellow, is grateful for a grant from the National Institute of General Medical Sciences (F32GM077940) for support. This work was also supported in part by a grant from the National Science Foundation (CHE 05−14056) to D.T. D.L.P. and D.T. also wish to acknowledge the National Energy Research Scientific Computing (NERSC) Center for providing computational time and resources.

Supporting Information Available: Plots of all possible radial distribution functions between TMAO and 5GP heavy atoms are provided along with the free energy profiles used to determine the T_m's of the different CG hairpin models. Also included are a set of tables which provide distances at which the potentials have been force-shifted to zero. Finally, a table giving estimates of ΔT_m for the 16-nt hairpin used in the LD experimental study[19] in the presence of various osmolytes is provided. This material is available free of charge via the Internet at http://pubs.acs.org.

JA078326W